Master Project – Spring 2010

Solar disinfection of viruses: role of carbonate radicals

Submitted by : Qingxia Zhong
Master of Environmental Sciences and Engineering (SIE)
Ecole Polytechnique Fédérale de Lausanne (EPFL)

Supervisor : Prof. Tamar Kohn
Environmental Chemistry Laboratory (LCE)
Ecole Polytechnique Fédérale de Lausanne (EPFL)

June, 2010 Lausanne

Abstract

French :

Le manque de sources d'eau potable améliorées contribue à beaucoup de maladies d'origine hydrique provoquées par des pathogèenes incluant des virus, protozoaires, bactéries ou des vers. Il est essentiel de développer et promouvoir des traitements pour fournir de l'eau désinfecté. La lumière du soleil joue un rôle important dans la désinfection de virus par photolyse directe ou photolyse indirecte par des espèces de transition réactives tel que les radicaux carbonates.

Cette étude a montré que le radical carbonate peut être produit en utilisant du 4-carboxylbenzophenone (CBBP) comme sensibilisant pour réagir avec les ions carbonate/bicarbonate. La concentration en radical carbonate à l'état d'équilibre a été déterminée en mesurant la dégradation d'un composé standard par chromatographie liquide (HPLC). La 4-nitroaniline s'est avérée être un composé standard approprié pour cette méthode. La concentration de CBBP a été variée pour générer les différentes concentrations en radicaux carbonates et ainsi de varier le taux d'inactivation des viruses. La concentration en radical carbonate mesurée variait entre 10^{-14} et 10^{-12} M correspondant aux valeurs obtenues lors d'études précédentes. L'étude cinétique de l'inactivation résultante a montré que l'ordre de réaction du radical carbonate était 0.13±0.064. Cet ordre était plus bas qu'on a prévu, ce qui peut être dû à la réaction de surface ou à l'interférence de 4-NA. La constante de ce pseudo-premier-ordre d'inactivation de Phi-X174 bacteriophage était 5 fois plus petite que celle de MS2. Le bacteriophage GA avait une constante d'inactivation semblable à MS2.

English:

Lack of improved drinking water sources contributes a lot to many waterborne diseases caused by pathogens which include viruses, protozoa, bacteria or worms. It is essential to develop and promote treatment methods in order to provide pathogen-free safe drinking water. Sunlight plays an important role in disinfection of viruses through direct photolysis or indirect photolysis through reactive transient species such carbonate radical.

This study demonstrated that carbonate radical can be generated using 4-carboxylbenzophenone (CBBP) as sensitizer to react with carbonate/bicarbonate ions. The steady state concentration of carbonate radical was determined by measuring the degradation of probe compounds using HPLC. 4-nitroaniline proved to be an appropriate probe compound to be used in this method. CBBP concentration was varied in order to generate different carbonate radical concentrations and subsequently vary the inactivation rate. The measured carbonate radical concentration varied from 10^{-14} to 10^{-12} M which corresponded to the values obtained from previous studies. The resultant inactivation kinetics showed that the reaction order of carbonate radical was 0.13±0.064 which may be due to the surface reaction or the interference of 4-NA. The pseudo-first order inactivation rate constant of Phi-X174 bacteriophage was 5 times smaller than that of MS2 while bacteriophage GA had similar inactivation rate constant with MS2.

Table of contents

Chapter I. Introduction

According to the WHO, 1.1 billion people have no access to any type of improved drinking water source. This leads to many waterborne diseases caused by pathogens which include viruses, protozoa, bacteria or worms. For example, there are 1.6 million deaths every year from diarrheal diseases and 133 million people who suffer from high intensity intestinal helminthes infections[2]. Lack of improved drinking water source contributes a lot in these problems. Therefore, it is essential to develop and promote treatment methods in order to provide pathogen-free safe drinking water[3].

Disinfection is physical or chemical process to eliminate or control the microorganisms in water that affect the water quality. Water and wastewater disinfection has experienced a tremendous development over the past decades. Common disinfection methods include the addition of chemical substances, ozone treatment, ultraviolet light, boiling and filtration etc. However, the lack of a reliable, effective treatment system is still a problem in many developing countries because of financial, educational or technological difficulties. A water treatment process that is relatively cheap and easy to run would be of inestimable value, especially for rural communities. Disinfection by solar energy is considered to be such a low-cost, effective, practical and simple alternative for water treatment processes. Because solar energy is universally available and free of charge, and because solar radiation can inactivate waterborne pathogens, sunlight-mediated disinfection is widely used. Besides, solar disinfection methods have other advantages such as that they form no harmful disinfection by-product[4], the process involves no transportation, storage or handling of chemicals, they are highly effective on a broad range of pathogens, and the hazard risk for operators is minimized.

1.1 Solar disinfection of water

Research on the effect of light upon bacteria and other organisms dates back to 1877, when Arthur Downe concluded that “light is inimical to the development of bacteria”[5]. The potential different sunlight-based water treatment processes have been further explored by various researchers throughout last century. Pioneering work toward the application of solar light for drinking water disinfection purposes was first conducted by Aftim Acra at the American University of Beirut in the early 1980s[6]. This work experienced a substantial follow-up by the research groups of Martin Wegelin at the Swiss Federal Institute of Aquatic Science and Technology (Eawag)[7] and Kevin McGuigan at the Royal College of Surgeons in Ireland[8].

Solar disinfection involves UV-B (290–320 nm), UV-A (320–400 nm), and visible light (400-700 nm) originating from the solar spectrum (Figure 1). The disinfection includes two different

processes: a direct germicidal effect caused by UV radiation and indirect photoinactivation which can be initiated by both UV and visible light[9]. Light in the UV-B range mainly acts by breaking the molecular bonds within micro-organismal DNA or RNA, producing thymine dimers in their nucleic acid, and thereby prohibiting growth and reproduction[10]. In addition, direct inactivation by UV-A light induces chemical or conformational changes of chromophores (light-absorbing components) within the cells[10]. This change leads to a loss of biological activity, culminating in the inactivation of the cell. UV-A is very efficient in inactivating bacteria, but viruses are typically not affected, since most viruses do not contain chromophores. Finally, infrared range also has a lethal effect on pathogens, by way of thermal disinfection[11]. The inactivation rate of microorganisms increases with decreasing wavelength[7]. The effectiveness of direct inactivation to inactivate different pathogen classes generally follows this sequence: protozoa> bacteria > viruses[12].

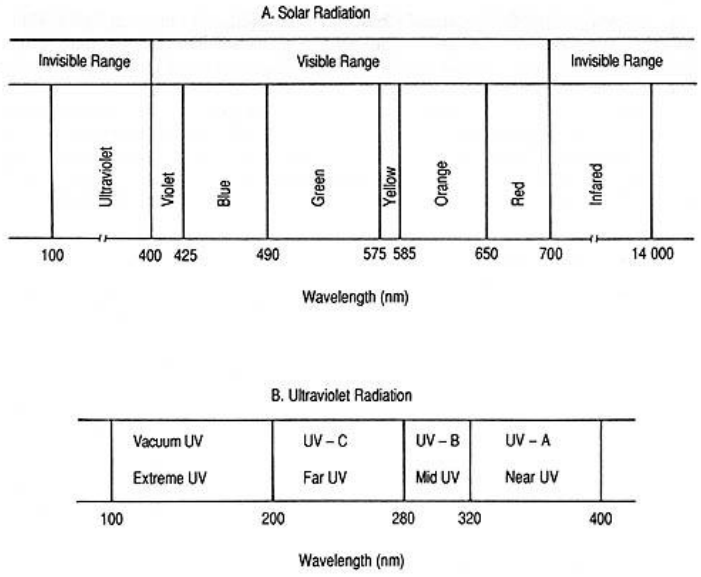

Figure 1. Spectra of nonionizing solar radiation (A) and ultraviolet radiation (B) showing main radiation bands, their nomenclature, and approximate wavelength limits. Other synonyms: UV-A, black light; UV-B, sunburn or erythemal radiation; UV-C, germicidal radiation[1].

Indirect disinfection can be divided into endogenous and exogenous photoinactivation. In both cases, the excitation of chromophores and subsequent reaction with oxygen leads to the formation of reactive oxygen species (ROS) that subsequently damage microorganisms by oxidizing cellular components [10, 11]. For endogenous inactivation, ROS are produced by cell-internal choromophores [10], while in the exogenous cases, chromophores located outside the organism, such as natural dissolved organic matter(DOM) that induce the photochemical reactions to create ROS [11].

1.2 Reactive Oxygen species (ROS) and carbonate radical

Reactive oxygen species (ROS) are transient species generated during radiation, respiratory burst, normal metabolic processes, etc[13]. In natural waters, one pathway of ROS formation is due to the interaction between DOM and molecular oxygen[14] upon absorption of solar energy. DOM is present in all natural or waste waters, and it consists of a complex mixture of molecules arising mainly from the decay of detritus. As a whole, DOM can absorb light over a considerable range of the sunlight spectrum, which makes it an environmentally important chromophore or sensitizer. ROS formed by the interaction of excited DOM and oxygen include superoxide anion ($O_2^-\cdot$), singlet oxygen ($^1O_2$), hydrogen peroxide (H_2O_2), hydroxyl radical (·OH), alkoxy (RO·) and peroxy ($RO_2\cdot$) radicals. Action of ROS on a cell can cause damage to the nucleic acid, oxidation of polysaturated fatty acids in lipids (lipid peroxidation), oxidation of amino acids in proteins, and inactivation of specific enzymes by oxidation of co-factors [15]. The more easily oxidizable the side chain of amino acids, the more readily they tend to react with ROS.

The carbonate radical is one of the radicals that are present in sunlit surface waters and in waters treated by advanced oxidation processes. Carbonate radical is not an ROS, but it is still an important transient species. It is strongly electrophilic which makes it a powerful oxidant towards electron-rich compounds such as anilines, phenols, and sulfur-containing compounds[16]. It has recently received much attention regarding its role in limiting the persistence of chemical pollutants. Carbonate radical was also reported to be capable of one-electron oxidation of several amino acids and proteins[17]. Lymar and Hurst[18] suggested that in phagosomes, which contain high levels of bicarbonate, the carbonate radical formed from scavenging of hydroxyl radicals might be a significant contributor to radical mediated damage.

In natural aquatic systems, the carbonate radical is formed by scavenging of the hydroxyl radical by carbonate and bicarbonate ion[19] following equation 1[20]. This reaction is particularly favorable in carbonate-rich waters (more than 1 x 10^{-3}M total carbon)[21].

$$\cdot OH + CO_3^{2-}/HCO_3^- \rightarrow CO_3^{\cdot-}/HCO_3^{\cdot} \quad (1)$$

Carbonate radical can also exist in its protonated form $HCO_3^{\cdot}$, but Bisby et al.[22] reported that this protonation does not occur in the pH range from 8 to 13. Besides via excited DOM, hydroxyl radical can be generated by photolysis of nitrate, nitrite and H_2O_2, or via (photo-)Fenton reaction[23-26] (Figure 2). The hydroxyl radical is a more powerful oxidizing reagent than the carbonate radical, as is evidenced by its higher one electron reduction potential[20]. Nevertheless, the steady-state concentration of carbonate radicals in natural waters is higher than that of hydroxyl radicals, since carbonate radicals react more selectively and consequently have a longer life time. The measured steady-state concentration of carbonate radicals was

found to be strongly dependent on light intensity and ranged from 5 x 10^{-15} to 10^{-13} M[27]. At this concentration, carbonate radicals are not directly measurable. Therefore, in order to measure their steady state concentration of carbonate radical, a probe compound is required which has high reactivity towards carbonate radical.

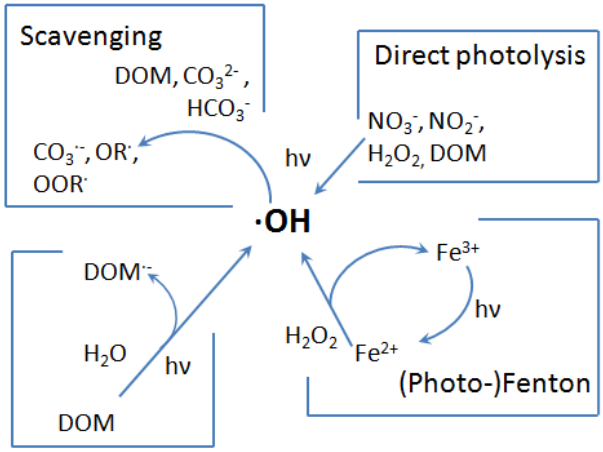

Figure 2. Sources of hydroxyl radical and production of carbonate radical in natural waters. (Adapted from Huang[20])

1.3 Viruses

A virus is a small infectious agent that can replicate only inside the living cells of an appropriate host. A virus consists of a core RNA or DNA, generally surrounded by a protein, lipid or glycoprotein coat, or some combination of the three[28]. There are several reasons that the study of viruses is important. First of all, viruses are the most abundant type of biological entity and they infect all types of organisms, from animals and plants to bacteria and archaea[29], potentially leading to serious or even deadly diseases. The number of known viruses now reaches over 5000 with new viruses being discovered frequently[28]. A vast number of waterborne viruses cause infectious diseases in humans. These diseases can be transmitted by the fecal oral route and infect their human hosts when drinking water sources are contaminated with untreated or insufficiently treated wastewater. For example, 10 million people in the world per year are affected by hepatitis which is an acute infectious disease of liver[30]. Hepatitis can be caused by at least five different viruses including hepatitis A and B[31]. This disease is most often transmitted by the fecal-oral route via drinking water. Essentially, it is vital to study viral diseases and virus disinfection. Other important waterborne viral infections include polyomavirus infection, gastroenteritis, SARS, etc[32-34]. Because of the important public health threat that viruses cause, studying viral diseases and disinfection is an essential task.

Secondly, most virus particles comprise a protein coat around their central core which makes them capsid or hydrophilic. And this protects the virus and makes it more resistant to

disinfectants; this protein coat also protects viruses from degradation by faecal organic material [35], thus viruses may survive for long periods in the environment. This makes the inactivation of viruses a big challenge.

1.4 Objectives

Many studies have been performed on the oxidation of organic compound by carbonate radicals. However, only a few have focused on viruses as the target. The goal of this project was to study the role of $CO_3^{\bullet-}$ in the disinfection of viruses, in order to assess the importance of this species during sunlight-mediated inactivation in general, and compared to inactivation by other ROS. Firstly, an experimental system had to be established that allowed us to study virus inactivation by $CO_3^{\bullet-}$. Subsequently, we aimed to quantify the disinfection kinetics, by investigating the dynamics of virus inactivation and simultaneously measuring the steady state carbonate radical concentration. Finally, we compared the susceptibility of different viruses toward disinfection by $CO_3^{\bullet-}$.

Chapter II. Experimental section

2.1 Organisms and reagents

Three bacteriophages are used in this project: MS2 (DSMZ 13767), PhiX-174 (DSMZ 4497) and GA (kindly provided by Laboratory of Water and Food Viral Pollution, Universitat de Barcelona) (Figure 3). Bacteriophages (phages) are viruses that specifically infect bacteria. MS2 is an RNA based icosahedral bacteriophage[36] with a diameter of 27-34 nm and it infects only male *E.coli* bacteria by injection of its RNA and A-protein[37]. MS2 was chosen for two reasons. Firstly, it is a common surrogate for human enteric viruses due to its similar size and morphology[38]. Secondly, the protein capsid of MS2 is unlikely to contain sensitizers that efficiently form ROS when exposed to sunlight[39]. Therefore, the endogenous inactivation by ROS can be excluded while studying the exogenous inactivation by $CO_3^{\bullet-}$. The second virus used was Phi-X174 bacteriophage which contains the first DNA-based genome to be sequenced[40]. Bacteriophage GA belongs to group II of the four serological groups of phages, infecting male *E. coli* bacteria[41]. Compared with MS2, the capsid protein sequence of GA has a 62% similarity of that of MS2 and a genomic sequence with 56.3% similarity with MS2[42]. The main difference between MS2 and GA is that GA coat protein does not have cysteine. The host for MS2, Phi-X174 and GA are *E.coli* DSMZ 5695, 13127, and 5695 respectively.

The viruses were propagated using *E.coli* as the host organism which was cultivated in LB medium, as described by Pecson et al., 2009[43]. The concentration of the MS2 stock solution was 3 x 10^{11} plaque-forming units (PFU)/mL, and viruses were stored in phosphate buffer since they are not stable in carbonate buffer. A plaque-forming unit (PFU) is a measure of the number of virus particles capable of forming plaques per unit volume. For example 1000 PFU/ml means that in one milliliter there are 1000 virus particles that are able to infect their host. Before each experiment, buffer exchange was performed during which the buffer solution was changed to 0.1 mM $NaHCO_3$ with 15 mM NaCl (pH 7.1) and the stock was diluted 40 times to 7.5 x 10^9 PFU/ml. Enumeration was performed using the double-layer agar method[44]. 0.1 ml of host *E.coli* and 0.1 ml diluted virus sample were mixed in an agar plate containing LB medium. The plate was placed in a 37°C incubator overnight. An example of an agar plate with MS2-infected *E.Coli* is shown in Figure 4.

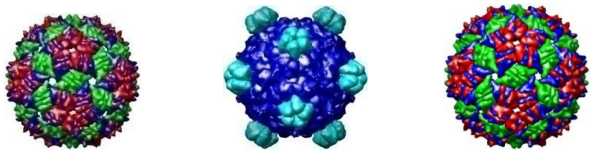

Figure 3. Capsid Images of Bacteriophage MS2, Bacteriophage Phi-X174 and Bacteriophage GA (from left to right) generated from ViPER virus capsid PDB files using the MultiScale extension to the Chimera interactive molecular graphics package[45].

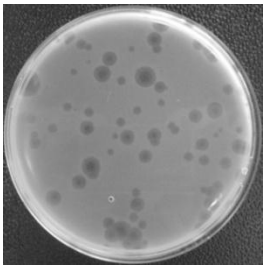

Figure 4. An agar plate done using double layer agar method. Phi-X174 bacteriophage was used to infect *E.coli*, and each circular plaque corresponds to an infection initiated by a single virion. Incubation time was 16 hours, 37°C.

Sodium bicarbonate ($NaHCO_3$, Aldrich, ≥99.5%), sodium phosphate dibasic dodecahydrate ($HNa_2O_4P.12H_2O$, Fluka, ≥ 99.0%), N,N-dimethylaniline ($C_6H_5N(CH_3)_2$, Fluka, ≥ 99.5%), 4-nitroaniline ($C_6H_6N_2O_2$, Fluka, ≥99%), 4-carboxybenzophenone ($C_6H_5COC_6H_4CO_2H$, Aldrich, 99%) acetonitrile (CH_3CN, Carlo Erba, ≥99.9% for HPLC), sodium azide (NaN_3, Fluka, ≥99.0%), Tris-EDTA buffer solution (Fluka, 10 mM Tris-HCl, 1 mM disodium EDTA, pH 8.0) and sodium chloride (NaCl, Acros Organics, ≥99.5%) were used as received. 18 MΩ cm deionized water was used throughout the course of the experiments.

2.2 Methods

2.2.1 Carbonate radical formation

Carbonate radical can be generated by various chemical reactions including scavenging of hydroxyl radical by carbonate and bicarbonate ions, or the oxidation of carbonate or bicarbonate by the sulfate radical anion (equation 2 and 3) or the excited triplet state of a sensitizer (equation 4 and)[46].

$$SO_4^{\cdot-} + HCO_3^- \rightarrow H^+ + SO_4^{2-} + CO_3^{\cdot-} \qquad k_{s1}=2.8 \times 10^6\ M^{-1}S^{-1} \quad (2)$$

$$SO_4^{\cdot-} + CO_3^{2-} \rightarrow SO_4^{2-} + CO_3^{\cdot-} \qquad k_{s2}=4.1 \times 10^6\ M^{-1}S^{-1} \quad (3)$$

$$^3Sens^* + HCO_3^- \rightarrow H^+ + \cdot Sens^- + CO_3^{\cdot-} \quad (4)$$

$$^3Sens^* + CO_3^{2-} \rightarrow \cdot Sens^- + CO_3^{\cdot-} \quad (5)$$

In this project, the sensitizer that was used to generate the carbonate radical was 4-carboxybenzophenone (Figure 5 left). It was chosen because it has been used as surrogates for excited triplet states of DOM. It induces oxidation of phenols and phenylurea herbicides and it is resistant to phtodegradation[46]. Under optical excitation, the aromatic ketone absorbs a photon and is promoted to its excited singlet state and further to excited triplet state by rapid

intersystem crossing in 10^{-7}s with a quantum yield near unity[47]. This triplet state is electron-deficient, so if its reduction potential is high enough, the triplet state ketone rapidly reacts with reducing agents like dissolved carbonate by electron transfer. Canonica et al.[46] tested the production of carbonate radical using this method at a Na_2CO_3 concentration of 500 mM and claimed that this reaction was predominant at high carbonate concentrations. The reduced product of ketone is the corresponding aromatic ketyl radical anion which is very unstable and easily goes back to ground-state by donating an electron to oxygen and producing superoxide radical anion (Figure 5 right).

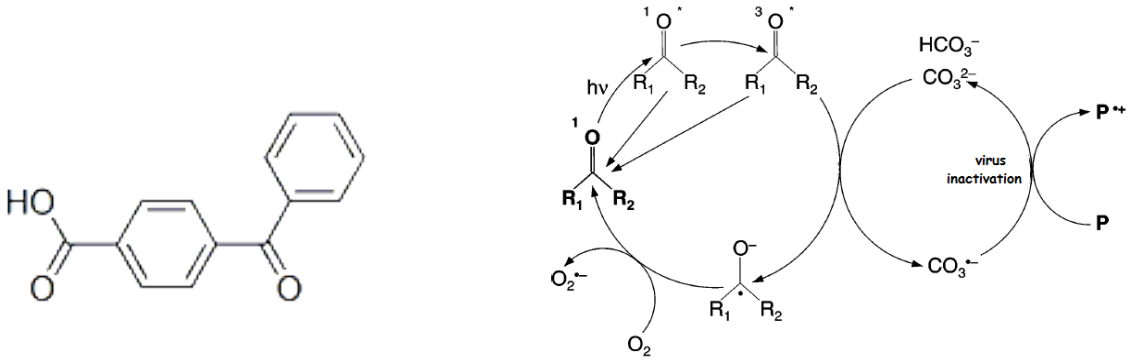

Figure 5. (left)Structure of 4-carboxybenzophenone and (right) the quenching of ^{3}CBBP* by carbonate/bicarbonate ions and the subsequent reaction of carbonate radical with probe. R_1: phenyl, R_2: 4-carboxyphenyl. (Adapted from Canonica et al.[46])

The second order rate constant for quenching of excited triplet states of CBBP by the carbonate ion is 1.3 x 10^6 $M^{-1}s^{-1}$, and that of bicarbonate ion was assumed to be 1 x $10^5 M^{-1}s^{-1}$. While the latter rate constant could not be determined with sufficient precision, it was found to be at least an order of magnitude lower than for carbonate[46]. CBBP has a pKa of 4.5, therefore, it was buffered with carbonate at pH 9.2 to have it more present in its charged, deprotonated form. This helped to increase its solubility in water. A solution containing 2.5 mM CBBP and 4 mM $NaHCO_3$ was mixed by sonication and stirring and was kept in a brown bottle in the refrigerator.

2.2.2 Measurement of steady state carbonate radical concentration

The carbonate radical concentration was assumed to stay at a steady state throughout the experiment. This concentration was measured by adding a probe compound and observing the depletion of this probe over time. Aniline derivatives are highly susceptible to electrophilic reactions, and were therefore used as probe compounds in this study. Two aniline derivatives were tested: N, N-dimethylaniline (DMA) and 4-nitroaniline (4-NA) which have second order reaction rate constants of $\boldsymbol{k_{aniline}}$ 1.8 x 10^9 and 6.3 x 10^7 $M^{-1}s^{-1}$ respectively[46] (Figure 6).

N,N-dimethylaniline

$C_8H_{11}N$

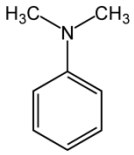

4-nitroaniline

$C_6H_6N_2O_2$

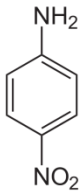

Figure 6. Chemical structures of the probe compounds used in this investigation

Aniline concentrations were monitored with HPLC. When plotting the $\ln(C/C_0)$ over time (equation 7), the slope is equivalent to the pseudo-first-order reaction rate constant k_{probe}^{obs}. From k_{probe}^{obs}, the steady state carbonate radical concentration can be calculated by dividing this k_{probe}^{obs} by k_{probe} (equation 9). The derivations are demonstrated in the following equations.

$$\frac{d[probe]}{dt} = -k_{probe}^{obs}[probe] \quad (6)$$

$$ln\frac{[probe]_0}{[probe]_t} = k_{probe}^{obs}t \quad (7)$$

where $$k_{probe}^{obs} = -k_{probe}[CO_3^{\cdot -}] \quad (8)$$

$$\therefore \quad [CO_3^{\cdot -}] = \frac{k_{probe}^{obs}}{k_{probe}} \quad (9)$$

2.2.3 Derivation of the inactivation equation

The next step is to relate the inactivation kinetics with steady state carbonate radical concentration. Assume that the inactivation of virus by carbonate radical follows equation 10 with a rate constant k_{virus} and a reaction order x on carbonate radical. The order on virus was taken to be 1 by assuming the carbonate radical concentration was constant during the inactivation. The viral inactivation curve was log-linear with respect to time (see Figure 13). This indicated that by taking carbonate radical as constant, the reaction is of pseudo-first-order.

$$r_{virus} = \frac{d[virus]}{dt} = -k_{virus}[CO_3^{\cdot -}]^x[virus]$$

$$= -k_{virus}^{obs}[virus] \quad (10)$$

$$k_{virus}^{obs} = \frac{r_{virus}}{[virus]} = k_{virus}[CO_3^{\cdot -}]^x \quad (11)$$

$$\therefore \quad logk_{virus}^{obs} = logk_{virus} + xlog[CO_3^{\cdot -}] \quad (12)$$

Several experiments have to be done in order to get a range of k_{virus}^{obs} and carbonate concentrations. The rate then simplifies to pseudo-first-order. Then by plotting $logk_{virus}^{obs}$ over $log[CO_3^{\cdot -}]$, x can be obtained from the slope while $logk_{virus}$ is the intercept. However, during the entire reaction, the rate data may be influenced by random sampling and analytical errors, potential contaminants that cause competing reactions, branching pathways and pH variations.

2.3 Experimental setup

Experiments were conducted in 100 ml batch reactors. The buffer solution used in this project were mainly carbonate buffers (6.5 - 100 mM $NaHCO_3$) with 10 mM NaCl. NaCl was used to provide a minimal ionic strength because viruses cannot survive at too low ionic strength[48]. Phosphate buffer (1 mM $Na_2HO_4P.12H_2O$ with 10 mM NaCl) was also used in order to do carbonate-free controls. The carbonate buffers used were sterile through 0.45µm filters, while the phosphate buffers were autoclaved. The glass reactors contained 50 ml buffer, 20 µl of a 7.5 x 10^9 PFU/ml virus stock solutions (final virus concentration of 3 x 10^6 PFU/ml). Furthermore, the solutions were spiked with CBBP at different concentrations which would be discussed in the following chapter, and with the aniline probes whenever the steady state carbonate radical concentration was measured. In addition, 2 µM EDTA was added in order to eliminate the possibility of trace metal-catalyzed oxidation. The pH was adjusted immediately before each experiment with NaOH and HCl to 9.2. For carbonate equilibrium and speciation calculations, closed system conditions were assumed, as the time necessary for equilibration with CO_2 in the atmosphere was longer than the duration of the experiment (< 3 hours). The closed system conditions were verified by adjusting the pH immediately before each experiment and re-measuring it immediately after each experiment, to confirm that the pH change was small compared to the change expected under open system conditions. As can be seen from the speciation diagram (Figure 7), the pH must be maintained at a high enough value in order to have a significant proportion of carbonate ions in solution. Such conditions are desirable since the carbonate has a much higher reactivity with ^{3}CBBP* than bicarbonate or bicarbonic acid. At the same time, there is an upper experimental limit since the viruses lose their infectivity at pH levels above 9[49].

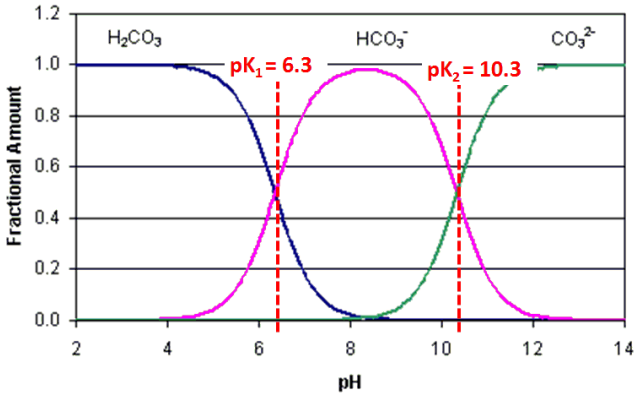

Figure 7. Concentration-pH diagram for a closed carbonate system

The reactors were exposed to simulated sunlight using a solar simulator (Abet Technologies, Sun 2000) with a collimated beam and a Xenon lamp. A UV-B/-C blocking filter (Abet) was used in order to eliminate wavelengths shorter than 320 nm (Figure 8). This was done to exclude the direct disinfection of virus by UV radiation. The irradiance that reached the reactors was 205 ± 2.17 W/m^2. The irradiance incident to different positions under the lamp was measured with a spectroradiometers ILT 900-R (InternationalLight Technologies, Massachusetts) and the variation was negligible. Dark controls of all the experiments were conducted under the same conditions, but the reactors were wrapped with aluminum foil. The reactors were placed in a water bath cooled to 20 °C by a recirculating water chiller (Julabo). A magnetic stirrer was placed under the water bath in order to provide a continuous stirring at 200 rpm. 120 µl aliquots were withdrawn at regular time intervals into 1.5 ml Eppendorf sampling tubes and stored in the refrigerator until further analysis. The sampling tubes were filled before sampling with 120 µl LB broth in order to buffer the pH. Another 1 ml samples were collected throughout the experiment into a 2 ml Amb.wide crimp top vial (Agilent Technologies) for HPLC analysis.

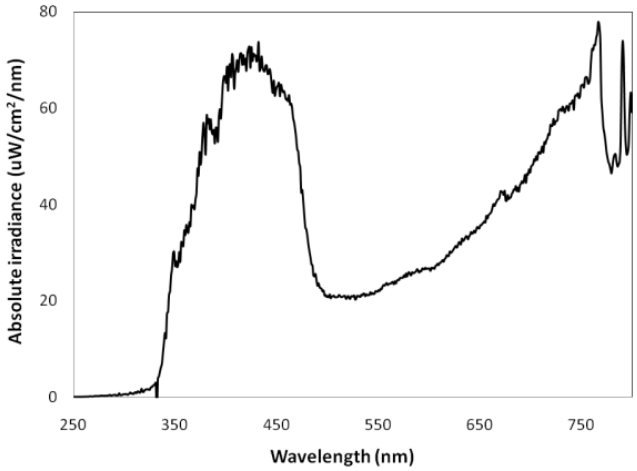

Figure 8. Solar simulator absolute irradiance measurement using spectroradiometer ILT 900-R (InternationalLight Technologies, Massachusetts) from 200 nm to 800 nm. UV-B/-C blocking filter was used which cut the light which wavelength shorter than 320 nm.

2.4 Data analysis

Probe compounds in the irradiated samples were directly analyzed by reverse-phase HPLC. Two HPLC series from Gracevydac were used: a series 1100 with single wavelength detection and a series 1050 with multi-wavelength detection function using a diode array detector (DAD). In both instruments, the same column was used (C18 column, 4.6 x 25 mm, 5µm) and isocratic conditions were carried out where compounds are eluted using constant mobile phase composition. Acetonitrile and deionized water was used as the HPLC solution in a 60:40 ratio at a flow rate of 1.0 ml/min. The spectrums of CBBP, DMA and NA were measured using a UV-Vis spectrophotometer (UV 2550, Shimadzu) as shown in Figure 9. Hence, the HPLC detection wavelengths were set correspondingly (Table 1). Because of its higher polarity, CBBP eluted before the aniline derivatives.

Table 1. HPLC conditions for compounds analyzed

Compound[a]	Detection wavelength (nm)	Retention time (min)
CBBP	264	2.60[b]
DMA	252	5.00[b]
NA	380	3.32[b]
NA	380	4.43[c]

[a] CBBP = 4-carboxybenzophenone; DMA = N,N-dimethylaniline; NA = 4-nitroaniline.
[b] Measured using HP series 1050
[c] Measured using HP series 1100

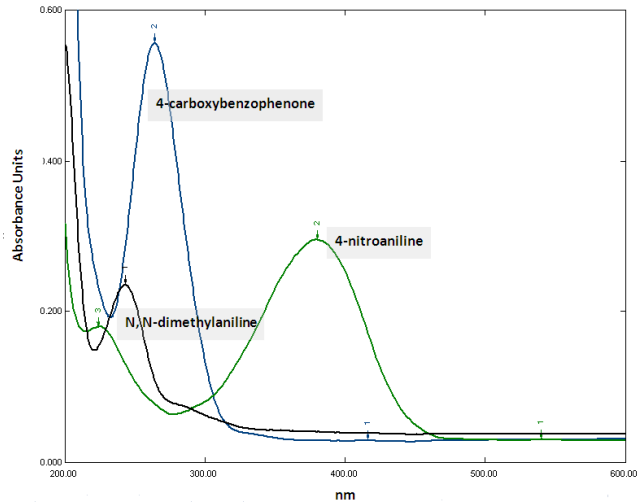

Figure 9. UV-visible absorption spectra for N, N-dimethylaniline, 4-carboxybenzophenone and 4-nitroaniline, recorded from 200 to 600 nm.

Chapter III. Results and discussion

3.1 Phase one: Selection of probe compound

Two aniline derivatives were tested regarding their potential to be used as probe compound. In order to determine the steady state carbonate radical concentration with the probe compound, it is essential that the radical consumption by the probe is insignificant compared to the total carbonate radical concentration. In this way, the system is not influenced by the presence of the probe compound. The impact of the probe compound on the steady-state radical concentration can be examined in two experiments with same conditions but different initial concentrations of aniline (5 µM and 10 µM). If the impact was not important, we would get the same steady-state carbonate radical concentration from both reactors, since they contained the same ketone and carbonate concentrations. N, N-dimethylaniline was first used. Figure 10 shows the depletion rate of N, N-dimethylaniline (DMA) at initial dose of 5 and 10 µM. The calculated carbonate radical concentrations were 2.04 x 10^{-13} M for 5 µM initial DMA and 1.87 x 10^{-13} M for 10 µM. By doubling the aniline concentration, the measured carbonate radical concentration decreased by 8%. Therefore, the lowest possible DMA concentration was used to minimize its impact on the accuracy of this method.

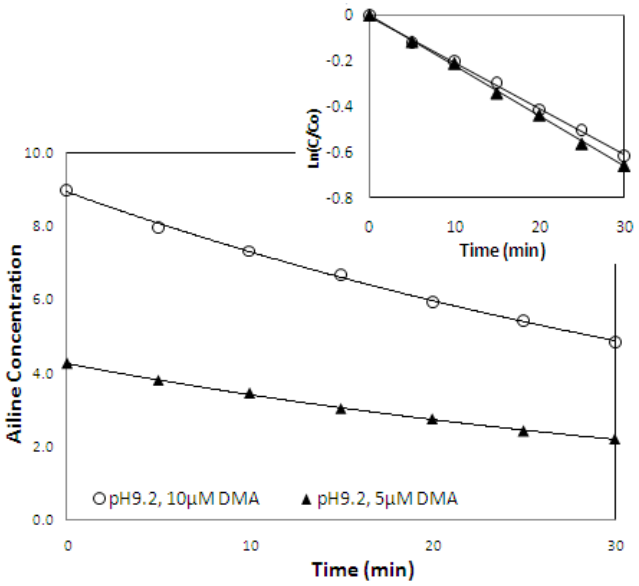

Figure 10. N,N-dimethylaniline depletion over time in aqueous solution containing 100 mM $NaHCO_3$ and 25 µM 4-carboxybenzophenone (pH 9.2), under constant irradiation. Two different initial concentrations of aniline were tested: ▲: 5 µM DMA; O: 10 µM DMA.

In addition, it was found out that with the presence of DMA in the solution, the inactivation of viruses became 20 times slower which again indicated that DMA played an important role in consuming carbonate radical. Experiments were done to compare the aniline decay with and without viruses present in the solution. The results were in agreement with the previous studies done by Huang who suggested that microorganisms were not responsible for the DMA

decay. Huang therefore concluded that the virus did not influence the steady-state concentration of the radical[27]. It was concluded that the higher DMA decreased steady state radical concentration and subsequently decreased the virus inactivation. However, the presence of virus alone does not influence the radical concentration.

The fraction of carbonate radical reacting with virus and DMA can be expressed as follows:

$$\frac{r_C^{MS2}}{r_C^{DMA}} = \frac{k_{virus}[virus][CO_3^{\cdot -}]^x}{k_9\ [DMA][CO_3^{\cdot -}]} \quad (13)$$

where r_C^{virus} and r_C^{DMA} represent the consumption rate of carbonate radical by virus and DMA respectively. k_{virus} is the inactivation rate constant and k_9 is the rate constant for the degradation of DMA by carbonate radical as indicated in Table 2.

Therefore, to get a good measurement of carbonate radical concentrations while simultaneously achieving significant virus inactivation, we had to either increase the virus concentration and decrease the DMA concentration or use another probe compound that has less reactivity towards the carbonate radical. However, the DMA concentration could not be lowered further due to the constraints of HPLC series 1050 multi-wavelength detector. The signal accuracy significantly decreased when the sample DMA concentration was less than 5 µM. Due to all the shortcomings of DMA, the probe compound was changed to 4-nitroaniline. Compared to DMA, 4-nitroaniline is less reactive towards carbonate radical because of the absence of methyl groups that act as electron donors. The second order rate constant for the reaction with carbonate radical is 6.3 x 10^7 $M^{-1}s^{-1}$[46] which is 30 times lower than that of DMA.

Virus inactivation experiments were performed in the presence of 4-nitroaniline. The results showed that the presence of 4-nitroaniline still inhibited MS2 inactivation. For comparison, the observed MS2 inactivation rates in the presence of 10 µM DMA, 10 µM 4-nitroaniline and no aniline were 0.013, 0.241, 0.797 min^{-1} respectively. However, the inhibition of MS2 inactivation by 4-nitroaniline was sufficiently small to allow us to measure both virus inactivation and carbonate radical within a reasonable time period. The HPLC signal for 4-nitroaniline was stronger than dimethylaniline at the same concentration. Furthermore, a series 1100 HPLC with single wavelength detection was used which had a higher accuracy and this made the measurement more reliable.

3.2 Phase two: Controls and corrections

The ultimate goal was to measure the carbonate radical effect. However, the system was very complex and there were many unaccounted for processes that might contribute to both virus inactivation and aniline probe compound degradation. All the possible processes in the system

are demonstrated in Figure 11. Therefore, to focus on carbonate radical contribution, before conducting experiments to quantitatively study the inactivation process and the steady state carbonate radical concentration, we first had to determine if other species are important, and if so, figure out how to separate their contribution from carbonate radical. And then assumptions could be made in order to simplify the system. Control experiments were performed in order to correct the values obtained from experiments, and to prove that the assumptions made throughout the experiments were necessary and reasonable. When Huang[27] did the carbonate radical concentration measurement using DMA as the probe compound, he suggested that microbial degradation, hydrolysis, or other non-photolytic oxidation reactions were not responsible for the observed DMA degradation by running DMA in dark. He also did carbonate free experiment in order to preclude the contribution of other photo-induced transients such as hydroxyl, alkoxy, and organoperoxyl radicals on DMA degradation. So we could expect a not so important error in our system.

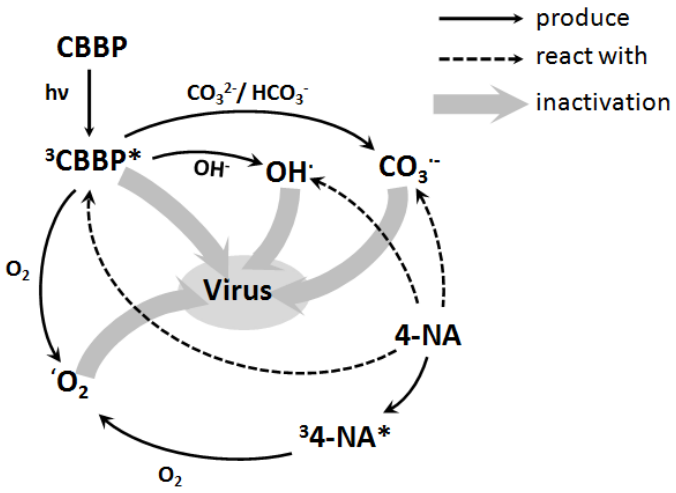

Figure 11. Potential reactions in the system that influence the results of our study of virus inactivation and steady state carbonate radical measurement.

3.2.1 Species in the system that could influence experiment results

3.2.1.1 Singlet oxygen

4-^{3}CBBP* does not react only with carbonate, but can also react with oxygen to produce singlet oxygen. Canonica reacted 50 µM CBBP with 500 mM carbonate at pH 11.0 using 308 nm laser pulses and he found out that the yield of $CO_3^{\cdot-}$ was approaching unity[46]. According to study of Wilkinson et al.[50], the corresponding singlet oxygen quantum yield of $^1O_2$ from benzophenone in methanol is less than 0.50. Therefore, it was assumed that the yield from 4-CBBP in water solution is also no more than 0.50. The relative production of $CO_3^{\cdot-}$ and $^1O_2$ from 4-^{3}CBBP* was calculated taking the saturated dissolved oxygen of 9.1 mg/L and CO_3^{2-} of 1.18 x

10^{-2} M for 100mM $NaHCO_3$ at pH 9.2. The resultant production of $CO_3^{\cdot-}$ is 70 times higher than that of $^1O_2$ as calculated below:

$$R = \frac{\Phi_C([CO_3^{2-}]+[HCO_3^-])}{\Phi_O[O_2]} \quad (14)$$

Where R is the relative production ratio of carbonate radical and singlet oxygen, Φ_C and Φ_O are the yields of carbonate and oxygen, respectively, i.e., the fraction of the reactants that is used to produce carbonate radical or singlet oxygen.

It was also reported that 4-nitroaniline was able to undergo the same photosensitized excitation as CBBP to produce ^{3}4-NA* which could eventually react with oxygen to produce singlet oxygen[51, 52]. The intersystem crossing efficiency of p-NA in water is much lower than that of CBBP (0.03[51] versus ~1[53]), but the second order rate constant of singlet oxygen generation from ^{3}4-NA* is almost 4 orders of magnitudes higher[52] than carbonate radical generation from carbonate and ^{3}CBBP*. Thus, the overall generation of $^1O_2$ could be important. Singlet oxygen is a very strong oxidant and it inactivates MS2 with a rate of 4 logs in 30 min [73].

One possibility to limit the effect of singlet oxygen is to add a quencher such as, NaN_3. To test the importance of singlet oxygen, 18.44 mM of NaN_3 was added to solution while keeping other variables unchanged. Theoretically, if azide selectively reacts with singlet oxygen and if singlet oxygen inactivates viruses, then the addition of azide would decrease the inactivation rate. However, the results showed a higher inactivation in the presence of azide. This agreed well with the studies done by Huie[54] who reported that azide not only quenched singlet oxygen, but also reacted with the carbonate radical to produce an azide radical (equation 15, second order constant of 1.3 x $10^7 M^{-1}s^{-1}$.). This new azide radical could then potentially inactivate the viruses, though this possibility was not explored in this project. As a result, azide was not used to do singlet oxygen control experiment.

$$CO_3^{\cdot-} + N_3^- \rightarrow CO_3^{2-} + \cdot N_3 \quad (15)$$

3.2.1.2 Hydroxyl radical

4-^{3}CBBP* can also react with hydroxyl ion to form hydroxyl radicals with a k equals to 1 x 10^7 $M^{-1}s^{-1}$[46]. It was necessary to check the relative importance of hydroxyl radicals compared to carbonate radicals. This was done by assuming steady state condition, and considering a system without virus:

$$\frac{d[CO_3^{\cdot-}]}{dt} = k_1[CO_3^{2-}]\left[{}^3CBBP^*\right] + k_2[HCO_3^-]\left[{}^3CBBP^*\right] + k_5[CO_3^{2-}][\cdot OH] + k_6[HCO_3^-][\cdot OH] - k_3[CO_3^{\cdot-}][4-NA] = 0 \quad (16)$$

$$\frac{d[\cdot OH]}{dt} = k_4[OH^-]\left[{}^3CBBP^*\right] - k_5[CO_3^{2-}][\cdot OH] - k_6[HCO_3^-][\cdot OH] - k_7[4-NA][\cdot OH] = 0 \quad (17)$$

$$\text{so} \qquad [\cdot\text{OH}] = \frac{k_4[OH^-]\left[{}^3CBBP^*\right]}{k_5[CO_3^{2-}] + k_6[HCO_3^-] + k_7[4-NA]} \quad (18)$$

$$and \qquad [CO_3^{\cdot-}] = \frac{(k_1[CO_3^{2-}] + k_2[HCO_3^-])\left[{}^3CBBP^*\right] + (k_5[CO_3^{2-}] + k_6[HCO_3^-])[\cdot OH]}{k_3[4-NA]}$$

$$= \frac{(k_1[CO_3^{2-}] + k_2[HCO_3^-] + \frac{(k_5[CO_3^{2-}] + k_6[HCO_3^-])k_4[OH^-]}{k_5[CO_3^{2-}] + k_6[HCO_3^-] + k_7[4-NA]})\left[{}^3CBBP^*\right]}{k_3[4-NA]} \quad (19)$$

Table 2. Rate constants in the reactions between different reagents in the system ($M^{-1}s^{-1}$).

Reagents	CO_3^{2-}	HCO_3^-	$CO_3^{\cdot-}$ (x 10^7)	$\cdot OH$ (x 10^8)	OH^-	$^1O_2$
${}^3CBBP^*$	1.3 x 10^6[46] **(k_1)**	1.0 x 10^5[46] **(k_2)**			1.0 x 10^7[46] **(k_4)**	< 0.50[b][50]
4-NA			6.3[46] **(k_3)**	100 [55]**(k_{10})**		
^{3}4-NA*						9.8 x 10^9[52]
DMA			185[46]**(k_9)**	140[16]**(k_7)**		
CO_3^{2-}				3.7[56]**(k_5)**		
HCO_3^-				0.085[56]**(k_6)**		

[a] the rate constant for HCO_3^- is at least one order of magnitude lower than that of CO_3^{2-}, here it is assumed to be 1.0 x 10^5
[b] quantum yield of singlet oxygen from 4-CBBP in methanol.

So the ratio of steady state carbonate radical concentration and hydroxyl radical concentration could be calculated for a solution at a given pH containing 100 mM total carbonate and 5 µm 4-nitroaniline. At pH 9.2, this ratio is 9.55 x 10^5, i.e., the hydroxyl radical concentration was negligible compared to carbonate radical in the solution. Furthermore, in order to distinguish between 4-NA degradation by ·OH and $CO_3^{\cdot-}$, the relative proportion of 4-NA that reacts with carbonate radical and with hydroxyl radical were estimated:

$$\frac{r_{4-NA}^C}{r_{4-NA}^{OH}} = \frac{(\frac{d[4-NA]}{dt})_C}{(\frac{d[4-NA]}{dt})_{OH}} = \frac{k_3[CO_3^{\cdot-}][4-NA]}{k_{10}[\cdot OH][4-NA]} = \frac{k_3[CO_3^{\cdot-}]}{k_{10}[\cdot OH]} \quad (20)$$

where r_{4-NA}^{C} and r_{4-NA}^{OH} are the aniline consumption rates over time. The calculated value of this ratio was 6.02 x 10^3 at pH 9.2 using k_3 = 6.3 x 10^7 $M^{-1}s^{-1}$ and k_{10} = 10^{10} $M^{-1}s^{-1}$(Table 2). Although the hydroxide anion is more efficient as a quencher the overall effect of the hydroxyl radical on nitroaniline decay is negligible which was in agreement with previous studies[46].

3.2.1.3 Triplet state ketone

Triplet state ketone is an oxidant because of its high standard one-electron reduction potential[57], so it could potentially inactivate viruses. Furthermore, Canonica has already reported that 4-^{3}CBBP* was able to directly cause the depletion of DMA[57]. Therefore, it must also be corrected from the observed viruses inactivation rate and aniline probe decay rate.

3.2.1.4 Other uncertainties

There could also be some other unknown impurities in the system that possibly contribute to virus inactivation and aniline decay.

Lilie [58]reported that carbonate radicals react with themselves to produce CO_2 and CO_4^{2-}. The carbonate radical concentration is of an order of 10^{-13}. Thus, even assuming that the rate constant of this self decay of carbonate radical is as high as 10^{10} $M^{-1}s^{-1}$, the resulting self consumption is small. This process does not influence our results.

3.2.2 Control experiments

In order to eliminate the effects of singlet oxygen, triplet state CBBP and all the other uncertainties on the measurements, decarbonation was done. The experiments were done in phosphate buffer where $NaHCO_3$ was replaced by 1 mM $Na_2HO_4P.12H_2O$. The triplet relaxation rate constant for ^{3}CBBP* is 6.7 x 10^5 s^{-1}[59]. If we compare the consumption of ^{3}CBBP* by carbonate/bicarbonate ions and by self relaxation as in equation 21:

$$\frac{k_1[CO_3^{2-}] + k_2[HCO_3^-]}{k_{self\ relaxation}}$$

$$= \frac{1.3 \times 10^6 M^{-1}s^{-1} \times 1.18 \times 10^{-2} M + 1.0 \times 10^5 M^{-1}s^{-1} \times 7.74 \times 10^{-2} M}{6.5 \times 10^5\ s^{-1}}$$

= 3.55% (21)

This indicates that the reaction of triplet ketone with carbonate is not important compared to its self relaxation. This means that ^{3}CBBP* is not affected by the presence of carbonate, and

therefore he production of singlet oxygen is not effected either. As a result, we could use the results from experiments performed in phosphate buffer to correct the data we obtained in carbonate buffer. The only parameter that changes from the phosphate to the carbonate buffer and between the different carbonate concentrations is the carbonate radical concentration.

Recall that the pseudo-first order inactivation of virus:

$$\frac{d[virus]}{dt} = -k_{virus}^{obs}[virus]$$

$$= -k_{virus\_C}^{obs}[virus] - k_{virus}^{obs\prime}[virus] \quad (22)$$

Where $k_{virus\_C}^{obs}$ represents the inactivation rate by only carbonate radical while $k_{virus}^{obs\prime}$ includes inactivation by all the other species, mainly triplet state CBBP and singlet oxygen.

$$\therefore \quad k_{virus}^{obs} = k_{virus\_C}^{obs} + k_{virus}^{obs\prime} \quad (23)$$

$k_{virus}^{obs\prime}$ could be obtained by doing phosphate experiments, and then the 'real' inactivation rate $k_{virus\_C}^{obs}$ is the difference between the rate in carbonate buffer and in phosphate buffer. Similarly, the $\mathrm{k}_{4-\mathrm{NA\_C}}^{\mathrm{obs}}$ represents the 4-NA decay attributed only to carbonate radical, and could be calculated by:

$$k_{4\_NA}^{obs} - k_{4\_NA}^{obs\prime} = k_{4-NA\_C}^{obs} \quad (24)$$

The correction experiments were done in 1 mM phosphate buffer with different CBBP concentrations ranging from 5 to 25 µM. The results presented a similar contribution of carbonate radical over total 4-NA decay (Table 3).

Table 3. Observed 4-nitroaniline (4-NA) decay rate in solution containing carbonate and phosphate buffer, with varied CBBP concentrations. $k_{4\_NA}^{obs}$ is the rate in 100 mM carbonate buffer, $k_{4\_NA}^{obs\prime}$ is the rate in 1 mM phosphate buffer and $k_{4\_NA\_C}^{obs}$ represents the rate that is due to carbonate radical. $k_{4\_NA}^{obs} - k_{4\_NA}^{obs\prime} = k_{4-NA\_C}^{obs}$. a and b are duplicate samples.

CBBP [µM]	$k_{4\_NA}^{obs}$ (x 10^{-6}) [min^{-1}]	$k_{4\_NA}^{obs\prime}$ (x 10^{-6}) [min^{-1}]	$k_{4-NA\_C}^{obs}/k_{4-NA}^{obs}$
5a	6.35	1.40	0.78
5b	5.65	1.45	0.74
12.5a	11.2	4.10	0.63
12.5b	10.9	2.92	0.73
25a	15.5	3.57	0.77
25b	12.9	2.01	0.84
		Average :	**0.75**

Table 4. Observed MS2 inactivation rate in solution containing carbonate and phosphate buffer, with varied CBBP concentrations. $k_{4\_NA}^{obs}$ is the rate in 100 mM carbonate buffer, $k_{4\_NA}^{obs\prime}$ is the rate in 1 mM phosphate buffer and $k_{4\_NA\_C}^{obs}$ represents the rate that is due to carbonate radical. $k_{4\_NA}^{obs} - k_{4\_NA}^{obs\prime} = k_{4-NA\_C}^{obs}$. a and b are duplicate samples.

CBBP [µM]	k_{virus}^{obs} (x 10^{-6}) [min^{-1}]	$k_{virus}^{obs\prime}$ (x 10^{-6}) [min^{-1}]	$k_{virus\_C}^{obs}/k_{virus}^{obs}$
5a	0.129	0.012	0.91
5b	0.133	0.013	0.90
12.5a	0.191	0.034	0.82
12.5b	0.175	0.037	0.79
25a	0.184	0.056	0.70
25b	0.194	0.06	0.69

In all the reactors with different CBBP concentrations, the observed 4-NA decay in phosphate buffer was 25% of that in carbonate buffer. This indicates that 75% of the 4-NA decay was due to carbonate radicals, so, in general:

$$k_{4\_NA\_C}^{obs} = 0.75 k_{4\_NA}^{obs} \quad (25)$$

For virus inactivation, the relative contribution between carbonate radical and the other reagents varied with changing CBBP concentration (Table 4).

The pseudo-first order inactivation rate constant in phosphate buffer increased linearly with increasing CBBP concentration while the trend in carbonate buffer was not linear. The ratio between the contribution from carbonate radical and the total observed rate ranged from 0.91 for lower CBBP concentration to 0.69 for higher CBBP concentration. This suggests that the contribution of virus inactivation due to carbonate radical over total inactivation rate decreased. The contribution from direct inactivation by ^{3}CBBP* and by singlet oxygen becomes more important in higher CBBP concentration. The ratio of $k_{virus\_C}^{obs}/k_{virus}^{obs}$ as a function of CBBP concentration was plotted (Figure 12), and this relation was used to correct virus inactivation rate.

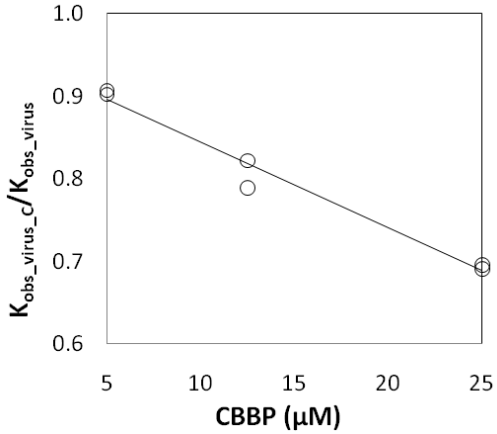

Figure 12. Changes in ratio of $k_{virus\_C}^{obs}/k_{virus}^{obs}$ with increasing CBBP concentration. (100mM carbonate, 5, 12.5 and 25µM CBBP, 5µM 4-nitroaniline and 1.5 x 10^7 PFU/ml MS2.)

3.3 Phase three: MS2 inactivation study

3.3.1 Effect of changing carbonate concentration on MS2 inactivation rate

In phase three, no aniline probe compound was added in the solution and only inactivation was studied. MS2 was used for all the experiments in phase three and four. Five experiments were conducted with different CBBP and $NaHCO_3$ concentrataions. In the first reactor, a solution containing 6.5 mM $NaHCO_3$ and 2.5 µM CBBP was added. In reactors 2, 3, and 4, 25 µM CBBP was used and the carbonate concentration varied from 25, 50 to 100 mM. Reactor 5 was the dark control and it had 100 mM carbonate and 25 µM CBBP as in reactor 4. The pH for all four reactors were adjusted to 9.2 prior to experiments. The virus concentrations were monitored during 2 hours.

Figure 13 shows MS2 inactivation in the five reactors. Hardly any inactivation was observed in reactor 1. The reason could be that not enough carbonate radicals were produced because of insufficient CBBP or carbonate. Carbonate and bicarbonate ion concentrations were calculated for the reactors 1-4 and results are shown in Table 5. In the system, there were hydroxyl radicals which degraded viruses and aniline probe compounds. High concentration of carbonate also increases the scavenging of hydroxyl radical and inhibit its effect. In addition, high carbonate also outcompetes all the other undesired oxidants such as singlet oxygen and other impurities. At pH 9.2 the ratio of CO_3^{2-} to HCO_3^- is 0.152, so the relative contribution of each ion on the reaction with CBBP is 1.98:1, as calculated in equation 26.

$$\frac{k_1[CO_3^{2-}][\,^3CBBP^*]}{k_2[HCO_3^-][\,^3CBBP^*]} = \frac{1.3\times10^6 M^{-1}s^{-1}\times1.18\times10^{-2}M}{1.0\times10^5 M^{-1}s^{-1}\times7.74\times10^{-2}M} \qquad (26)$$

$$= 1.98$$

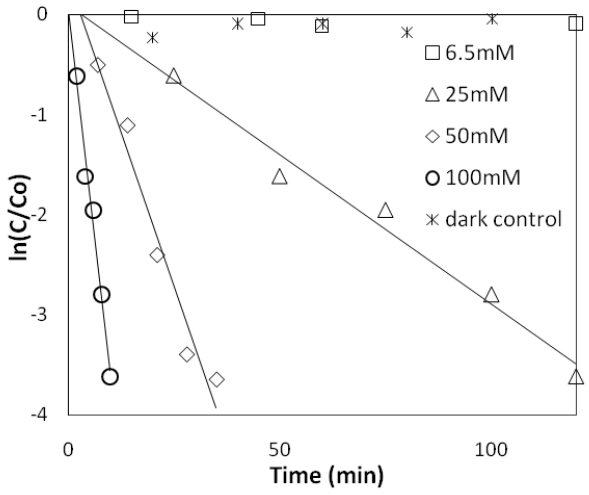

Figure 13. MS2 inactivation in carbonate buffer solution. Carbonate and CBBP concentrations were varied. Reactor one contained 6.5 mM carbonate and 2.5 µM CBBP. Reactors 2 to 4 contained 25 µM CBBP and 25, 50, 100 mM carbonate respectively. Reactor 5 was the dark control, and it contained 100 mM carbonate and 25 µM CBBP. The initial virus concentration was 1.5 x 10^7 PFU/ml. Samples were illuminated using the UV B/C filter. Values not corrected.

Table 5. Carbonate/bicarbonate ion concentration at pH 9.2 in closed system with different total carbonate (calculated using Visual Minteq.)

Total carbonate (mM)	CO_3^{2-} (mM)	HCO_3^- (mM)
100	1.18×10^{-2}	7.74×10^{-2}
50	5.47×10^{-3}	4.11×10^{-2}
25	2.53×10^{-3}	2.13×10^{-2}
6.5	5.92×10^{-4}	5.75×10^{-3}

By decreasing the total carbonate from 100 mM to 50 mM, and to 25 mM, inactivation rates decreased from 0.27±0.02 min^{-1} (4 logs inactivation in roughly 10 minutes) to 0.09±0.01 min^{-1} (4 logs in 40 minutes), and to 0.022±0.002 min^{-1} (4 logs in more than 120 minutes). This indicates that carbonate played a major role in this inactivation since for the three cases, carbonate concentration was the only changing parameter. It was observed that no inactivation occurred in the dark control as expected since no ^{3}CBBP* was produced without photoexcitation, and consequently no radical was produced to cause inactivation.

The experiment was repeated with 25, 50 and 100mM $NaHCO_3$ and 25µM CBBP and the results are shown in Figure 14. There was a high level of variability between replicates, even though the experimental conditions were identical. This indicated significant variability in the system which may be due to the fact that the carbonate radical steady state concentration was very sensitive to sinks arising from impurities. However, in general there was a clear increase of the rate with increasing carbonate concentration. The average pseudo-first order inactivation rates for the three carbonate concentrations were 0.042±0.02 min^{-1} (25 mM), 0.17±0.13 min^{-1} (50 mM) and 0.37±0.23 min^{-1} (100 mM).

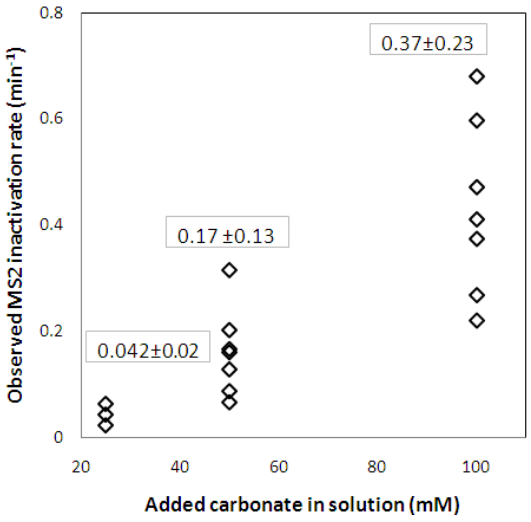

Figure 14. Pseudo-first order inactivation rate constants of MS2 as a function of carbonate concentration with 25 µM CBBP, pH 9.2. Three carbonate concentrations were applied (25, 50 and 100 mM) and tested in multiple replicates. Average values were marked. The rate values are corrected for the contribution of other species.

3.3.2 Effect of changing CBBP concentration on MS2 inactivation rate

For the following experiments, instead of changing the carbonate concentration in order to produce different steady state carbonate radical concentrations, the carbonate concentration was kept at 100 mM, but the CBBP dosage was varied. This new approach was chosen in order to minimize the importance of side reactions with other transient species. As mentioned above, this is best done by maximizing the carbonate concentration of the solution. Experiments were performed with varied CBBP concentration as already mentioned in section 3.2, and the $k_{virus\_C}^{obs}$ was plotted after correction for contribution from other species (Figure 15). The increase in the observed inactivation rate constant was linear.

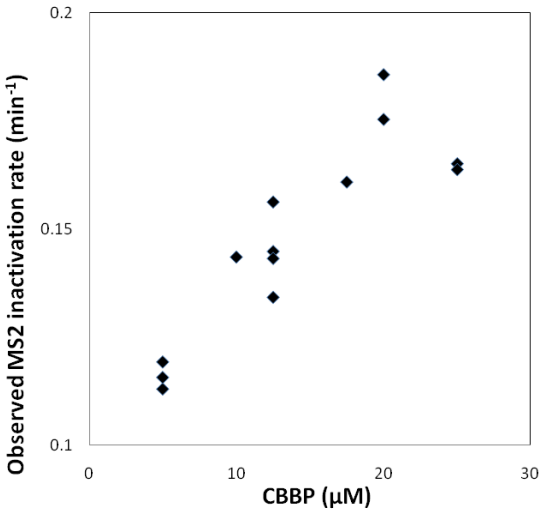

Figure 15. Pseudo-first order inactivation rate constants of MS2 vs added CBBP in the solution with 100 mM carbonate. Six CBBP concentrations were applied (5, 10, 12.5, 17.5, 20 and 25 µM) where each of them several duplicates were made. The rate values were corrected for the contribution from other species.

3.4 Phase four: measurement of steady state $CO_3^{\cdot-}$ concentration

In the phase four experiments, 5 µM 4-NA was added as a probe in the reactor with carbonate buffer, CBBP and virus, and samples were taken for HPLC analysis. The carbonate radical concentration was calculated as described previously and corresponded to 6.06 x 10^{-13} M (Figure 16).

3.4.1 Effect of pH on the measured $CO_3^{\cdot-}$ concentration

Experiments were also performed at different pH values to test the relative importance of the carbonate and bicarbonate ion concentrations in the formation of carbonate radicals. In theory, the higher the pH, the higher the fraction of carbonate ions, and hence more carbonate radical

would be produced. This hypothesis was supported by the results of these experiments (Table 6).

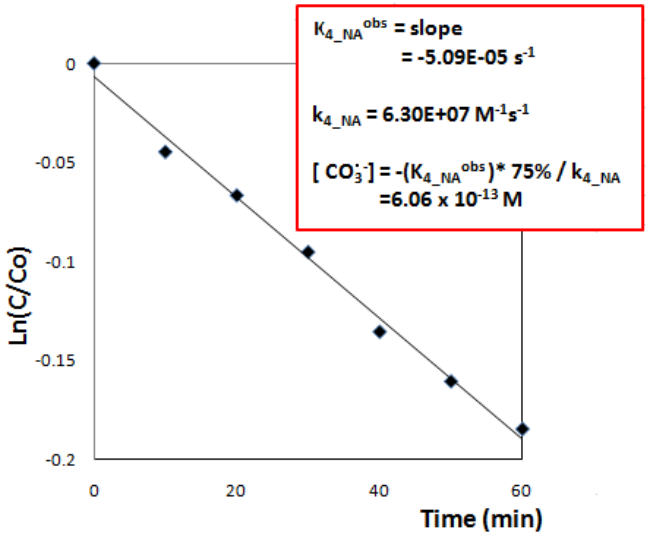

Figure 16. 4-nitroaniline depletion over time in aqueous solution containing 100 mM $NaHCO_3$, 25 µM 4-carboxybenzophenone and 5 µM 5-NA initially, under constant irradiation. pH9.2. Calculation of carbonate radical concentration is shown. The value was corrected for contribution of other species.

Table 6. Carbonate/bicarbonate ion concentrations at different pH with 100mM $NaHCO_3$ and 25µM CBBP and 10µM DMA, and the resulted carbonate radical concentration. Values were corrected for contribution of other species.

pH	CO_3^{2-} (mM)	HCO_3^- (mM)	$CO_3^{\cdot-}$ (M)
9.2	1.18 x 10^{-2}	7.74 x 10^{-2}	1.40 x 10^{-13}
9.4	1.69 x 10^{-2}	6.95 x 10^{-2}	1.65 x 10^{-13}
9.6	2.34 x 10^{-2}	5.98 x 10^{-2}	1.88 x 10^{-13}

3.4.2 Effect of changing carbonate concentration on the measured $CO_3^{\cdot-}$ concentration

In order to confirm the relation between carbonate/bicarbonate ion in the solution and the measurement of carbonate radical steady-state concentration, different carbonate concentrations were added to solution while keeping all the other experiment conditions the same. DMA was used in this experiment. The solution contained 5 µM DMA, 1.5 x 10^7 PFU/ml viruses and 25 µM CBBP (pH 9.2). The results are shown in Figure 17. The increase in measured carbonate radical concentration increases as the total carbon increased (9.85 x 10^{-14}, 1.55 x 10^{-13} and 2.03 x 10^{-13} M for 25, 50 and 100 mM carbonate buffer, respectively). However, this increase was less than 1:1.

It was observed from Figure 17 (b) that if we extend the trend line to a carbonate concentration of zero, the carbonate radical concentration was not zero. From this it could be concluded that the measured DMA depletion could not be entirely attributed to carbonate radicals. This, in

turn, implies that the steady state carbonate radical concentration was overestimated, as was discussed in section 3.2.

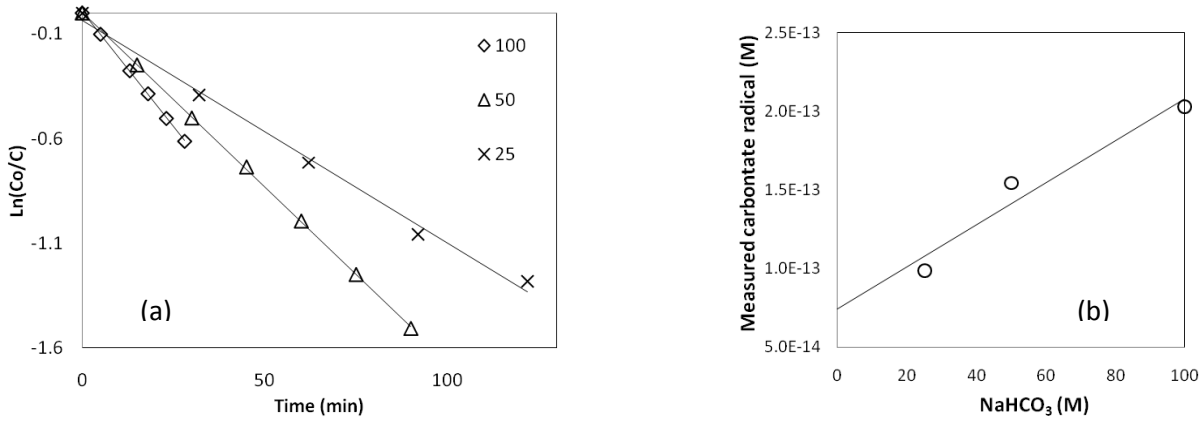

Figure 17. N, N-dimethylaniline decay over time (a) and the resultant carbonate radical concentration as a function of carbonate in the solution (b) with three different $NaHCO_3$ concentrations: 25, 50 and 100 mM. Values are corrected for contribution of other species.

3.4.3 Effect of changing CBBP concentration on the measured $CO_3^{\bullet-}$ concentration

Similar to inactivation experiments, the effect of changing the CBBP concentration on the measured carbonate radical concentration was also studied. The measured carbonate radical concentrations were plotted as a function of CBBP dosages. CBBP dosage was chosen as the independent variable, since the conversion of CBBP into triplet excited state is only related to irradiation and CBBP concentration. Therefore the variation in the amount of ground state concentration should correspond well to that of triplet state CBBP.

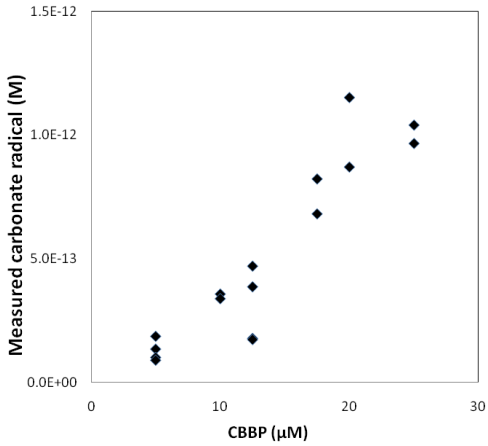

Figure 18. Measured carbonate radical concentration in the solution with same $NaHCO_3$ concentrations (100mM). Six different 4-carboxybenzophenone (CBBP) concentrations were used: 5, 10, 12.5, 17.5, 20, 25 µM. Values were corrected for contribution of other species.

The results showed a clear linear relation between the CBBP concentration and the resultant carbonate radical concentration. The trend looks similar as in Figure 15. It is observed from the graph that if there is no CBBP present, the measured carbonate radical is approaching zero.

3.5 Determination of MS2 inactivation rate equation parameters

After having conducted a series of MS2 inactivation and carbonate radical measurements, we could establish the relationship between the two simultaneous processes. As described in section 2.2.3., recall equation 10, while replace k_{virus}^{obs} and $[CO_3^{\cdot-}]$ by values that were corrected for the contribution of other species:

$$logk_{virus\_C}^{obs} = logk_{virus} + xlog[CO_3^{\cdot-}]$$

And $logk_{virus\_C}^{obs}$ was plotted against $log[CO_3^{\cdot-}]$ (Figure 19). From the data in Figure 19, the slope and intercept of the graph were obtained which corresponded to the log10 of the reaction order x and the log10 of $k_{virus.}$ The resultant x is 0.13±0.064 which is smaller than one. This is surprising since a reaction order of 1 or 2 was expected. For example, Kohn and Nelson [9] have reported second order disinfection kinetics of virus by singlet oxygen with a rate constant of 4.8 x 10^{12} ± 1.5 x 10^{12} $M^{-1}h^{-1}$. This reaction order that is less than one could be explained by a combination of reaction order zero and one. It is possible that the inactivation process involves more than one phase in the solution. One of them is the homogeneous process in the bulk solution , where the reaction order is 1. The other part of the reaction, on the other hand, is potentially a zero order reaction that involves diffusion and surface reaction. For example, a possible situation is that the production of carbonate radical by ^{3}CBBP* and carbonate/bicarbonate ions is of 1st order while the interaction between virus and the carbonate radical is zero order. The carbonate radical may reacts only when adsorbed to the virus surface. When the adsorption tendency is strong, the adsorption surface will be completely covered and the reaction rate will be independent of the concentration of radicals.

Another explanation could be that when the carbonate radical concentration reached a certain level, its effect on viruses disinfection did not increase linearly, either because a bigger portion of the radical reacted with 4-nitroaniline instead of viruses at high radical concentrations, or the radical became saturated in terms of reacting with viruses. This can also be seen from Table 4 and Figure 18, the former showed that with the increase of CBBP the portion of the rate constant that was due to carbonate radical reduced while the latter showed that this increase of CBBP did cause a proportional increase in the carbonate radical concentration. Therefore, although more carbonate radicals were generated, there were also more carbonate radicals reacting with 4-NA instead of viruses, because 4-NA was more competitive in terms of reactivity towards carbonate radicals. This change can also be seen in Figure 12, which shows that the

portion of rate constant attributed to carbonate radical over the entire rate constant decreased with the increase of CBBP dosage. At higher CBBP concentration, CBBP became more important in the inactivation of viruses.

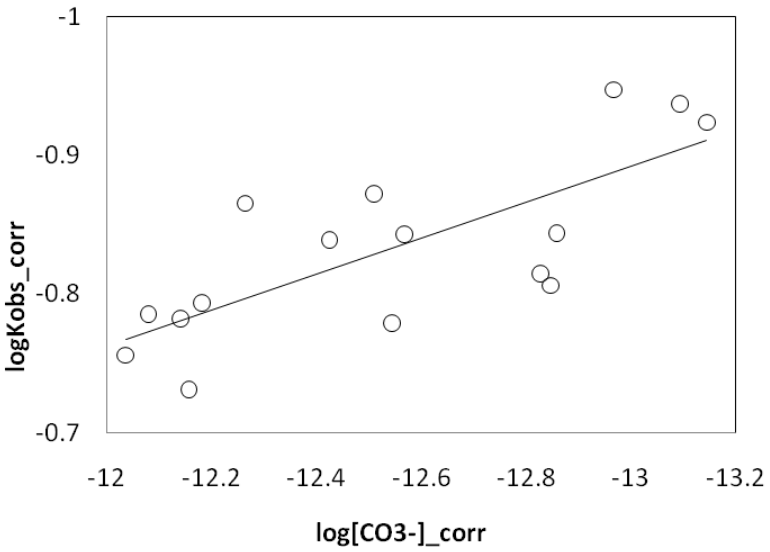

Figure 19. log10 of corrected pseudo-first order rate constant of MS2 inactivation by carbonate radicals over log10 of corrected carbonate radical concentration. 100mM carbonate, 5µM 4-nitroaniline, pH9.2.

3.6 . Comparison between inactivation of MS2, Phi-X174 and GA

In the last part of the study, a comparison was made to examine the susceptibility of different viruses toward disinfection by carbonate radical. In addition to MS2, experiments were performed under the same condition with Phi-X174 and GA (Figure 20). The probe compound was not added in these experiments. Because MS2 and Phi-X174 infects different *E.coli* bacteria, they can be added in the same reactor but the samples must be plated using different bacteria. MS2 and GA infect the same bacteria, therefore the comparison had to be done in separate reactors. Results showed that the observed inactivation rate constant of MS2 was 5 times larger than that of Phi-X174. Pecson et al.[43] have studied the inactivation of MS2 and Phi-X174 by hydroxyl radical and singlet oxygen and found that the inactivation rate constants of MS2 were 41.6 and 11.6 times larger than that of Phi-X174.

The difference between the inactivation of these two viruses might be due to different genomes, protein coat or isoelectric point. Firstly, if we compare the genome of MS2 and Phi-X174, MS2 has a single stranded RNA while Phi-X174 has a DNA genome. MS2 has a very small genome which is 3569 nucleotides long [60], however, Phi-X174 has a genome size of 5386 [40]. If the inactivation occurs in the genome of the viruses, MS2 would be more susceptible because of its simpler and smaller genome. In addition, the difference in amino acids also made the inactivation rate vary. If, on the other hand, the inactivation occurs on the protein capsid, the

difference in protein coats of the two viruses has to be studied. The isoelectric point of MS2 is 3.9 while that of Phi-X174 is 6.6[61]. Under the condition of this experimental pH of 9.2, MS2 would be more negatively charged and more favorable for oxidation by carbonate radical which is electron deficient. Compared to MS2, the potential of Phi-X174 to be oxidized is smaller because of its lower isoelectric point. Therefore, MS2 might has a faster inactivation rate. Phi-X174 was added also in the same reactor with MS2, and it was found that there was no observable competition, since the activation rate was equivalent to the case where the reactor contained only Phi-X174. On the other hand, GA is very similar to MS2. Experiment results showed that the two bacteriophages had the same pseudo-first order inactivation rate constant.

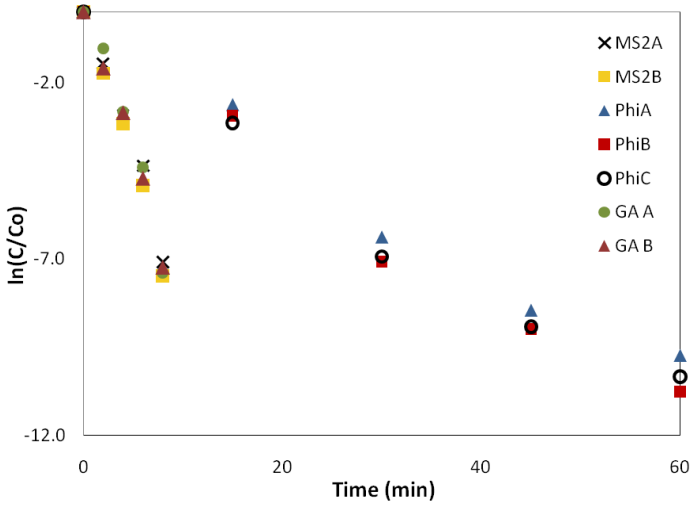

Figure 20. Inactivation of bacteriophage MS2, Phi-X174 and GA by carbonate radical over time. 100 mM $NaHCO_3$, 25 µM CBBP, no probe compound was added. A and B are replicates. For MS2 A, B and Phi-X174 A, B, MS2 and Phi were in the same reactor while reactor C only contained Phi-X174. For GA A, B, there was only GA in the reactor.

Same experiments were also performed in the presence of 5 µM 4-NA. The results showed that 4-NA inhibited the inactivation of all the three viruses. The rate constants were listed in Table 7.

Table 7. Inactivation rate constant (min^{-1}) of bacteriophage MS2, Phi-X174, GA by carbonate radical in 100 mM carbonate, 25 µM CBBP, with and without 5 µM 4-NA.

	MS2	Phi-X174	GA
Without 4-NA	0.88±0.030	0.24±0.0090	0.90
With 4-NA	0.24±0.0015	0.041	0.13

Hydroxyl radical has a reduction potential of 2.4 V[62], and singlet oxygen has a potential of 2.15. The reduction potential of carbonate radical is smaller (1.59V at pH12[22]). If we compare the inactivation of the same viruses by different transient species, theoretically the rate should follow hydroxyl radical > singlet oxygen > carbonate radical. However, the inactivation rate also depends on experimental conditions. Under different conditions, this order may change. Therefore, in order to compare the inactivation by different transient species, more experiments have to be done with the oxidant as the only variable.

Chapter IV: Conclusion

Viruses are threatening public health in both industrialized and developing nations. Effective water treatment options have to be developed in order to cope with viral infections. Solar disinfection was recognized as an effective, cheap and easy system. However, studies need to be done in order to understand better the processes leading to virus inactivation in solar disinfection. This study showed that carbonate radical plays an important role in solar disinfection of viruses. Carbonate radical was generated using 4-carboxylbenzophenone (CBBP) as sensitizer to react with carbonate/bicarbonate ions. The steady state concentration of carbonate radical was determined by measuring the degradation of probe compounds using HPLC. Two probe compounds were used: N, N-dimethylaniline (DMA) and 4-nitroaniline (4-NA). 4-NA proved to be a better probe compound in this study because it could enable both inactivation and carbonate radical concentration measurement. The reactivity of DMA toward carbonate radical was so high that the reaction between DMA and carbonate radical inhibited the inactivation process. CBBP concentration was varied in order to generate different carbonate radical concentrations and subsequently vary the inactivation rate. The resultant inactivation kinetics showed that the reaction order of carbonate radical was 0.13±0.064 which may due to the surface reaction or the interference of 4-NA. The inactivation of Phi-X174 bacteriophage was 5 times slower than that of MS2. And the inactivation of both viruses by carbonate radical was faster than inactivation by hydroxyl radical and singlet oxygen.

In natural waters, carbonate radicals are produced by the reaction of hydroxyl radicals with carbonates and bicarbonates, and also by the reaction of carbonates/bicarbonates with dissolved organic matters (DOM). The excited triplet state of DOM is a significant source of carbonate radicals in sunlit natural waters at pH values higher than 8[46]. For sunlit waters with high DOM the reactivity of carbonate radical could be important. In Greifensee, a eutrophic Swiss lake, the carbonate radical formation rate from DOM was reported to be $1 \times 10^{-14} Ms^{-1}$[46]. However, it should also be noted that DOM can also act as a carbonate radical scavenger, as the aniline derivatives did in this study [21]. Carbonate radicals can also be formed by hydroxyl radicals, which, in turn, are formed via several pathways. Hydroxyl radical itself is a very reactive oxidant; however, its environmental concentration is lower than carbonate radical due to its lower selectivity. Therefore, this makes the carbonate radical an even more important transient species in natural water. The importance of different transient species on the disinfection of water depends on the type of water and contaminants in the water.

Further studies can be done to understand where carbonate radical attacks the viruses and possible factors that promote or inhibit the inactivation. We could also study the inactivation of viruses by carbonate radical in natural waters and in wastewater treatment plants to compare the importance of carbonate radical with other transient species.

Acknowledgement

The project was done under help of project supervisor, Assistant Professor Tamar Kohn, with her wonderful support, kind guidance and valuable advice for this project. I received great support from Michael Mattle throughout the whole project. Without his guidance and suggestions this project could not be realized. I also thank Dr. Brian Pecson, Dr. Krista Rule Wigginton, Jessica Nieto, Therese Sigstam and Florence Bonvin from Environmental Chemistry Lab of EPFL for their great help during my stay in the lab. The lab assistance of Dominique Grandjean and Rebecca Rutler is much appreciated.

References

1. Acra, A., Jurdi, M., Mu'allem, H., Karahagopian, Y. and Raffoul, Z.,, *Water disinfection by solar radiation: Assessment and application*. 1989, The International Development Research Centre.
2. WHO. *Health through safe drinking water and basic sanitation*. 2010; Available from: http://www.who.int/water_sanitation_health/mdg1/en/index.html.
3. Jamil, Y., Ahmad, M.R., Ali, K., Habeeb, A. and Hassan, M, *Use of solar energy for disinfection of polluted water.* Soil & Environ, 2009. 28(1): p. 13-16.
4. Solsona, F.a.M., J.P., *Water disinfection*. 2003, Pan American Center for Sanitary Engineering and Environmental Sciences: Lima. p. 19.
5. Downes, A.a.B., T.P., *Researches on the Effect of Light upon Bacteria and other Organisms.* Proceedings of the Royal Society of London, 1877. 26: p. 488-500.
6. Acra, A., Raffoul, Z. and Karahagopian, Y., *Solar Disinfection of Drinking Water and Oral Rehydration Solutions-Guidelines for Household Application in Developing Countries*, UNICEF, Editor. 1984, Illustrated Publications: Amman.
7. Wegelin, M., Canonica, S., Meshcner, K., Fleischmann, T. Pesaro, F. and Metzler, A., *Solar water disinfection: scope of the process and analysis of radiation experiments.* Journal of Water Supply: Research and Technology - Aqua, 1994. 43(3): p. 154-169.
8. Conroy, R.M., et al., *Solar disinfection of drinking water and diarrhoea in Maasai children: A controlled field trial.* Lancet, 1996. 348(9043): p. 1695-1697.
9. Kohn, T. and K.L. Nelson, *Sunlight-mediated inactivation of MS2 coliphage via exogenous singlet oxygen produced by sensitizers in natural waters.* Environmental Science & Technology, 2007. 41: p. 192-197.
10. Dejung, S., et al., *Effect of solar water disinfection (SODIS) on model microorganisms under improved and field SODIS conditions.* Journal of Water Supply Research and Technology-Aqua, 2007. 56(4): p. 245-256.
11. Oates, P.M., P. Shanahan, and M.F. Polz, *Solar disinfection (SODIS): simulation of solar radiation for global assessment and application for point-of-use water treatment in Haiti.* Water Research, 2003. 37(1): p. 47-54.
12. Leinberger, J., *Disinfection of Drinking Water with Ultraviolet Light*, Trojan Technologies Inc.: Ontario.
13. Zhu, H.P., et al., *Transient species and its properties of melatonin.* Science in China Series B-Chemistry, 2006. 49(4): p. 308-314.

14. Helbling, E.W.a.Z., H., ed. *UV effects in Aquatic Organisms and Ecosystems*. Chapter 8: Reactive oxygen species in aquatic ecosystems, ed. D.J. Kieber, Peake, B.M. and Scully, N.M. 2003, The Royal Society of Chemistry: Cambridge. 251-288.
15. Lin, Z.D., et al., *Free methionine-(R)-sulfoxide reductase from Escherichia coli reveals a new GAF domain function.* Proceedings of the National Academy of Sciences of the United States of America, 2007. 104(23): p. 9597-9602.
16. Neta, P., R.E. Huie, and A.B. Ross, *Rate constants for reactions of inorganic radicals in aqueous-solution.* Journal of Physical and Chemical Reference Data, 1988. 17(3): p. 1027-1284.
17. Adams, G.E., et al., *Selective free-radical reactions with proteins and enzymes-reactions of inorganic radical anions with amino-acids* Radiation Research, 1972. 49(2): p. 278-&.
18. Lymar, S.V. and J.K. Hurst, *Role of compartmentation in promoting toxicity of leukocyte-generated strong oxidants.* Chemical Research in Toxicology, 1995. 8(6): p. 833-840.
19. Buxton, G.V. and A.J. Elliot, *Rate-constant for reaction of hydroxyl radicals with bicarbonate ions.* Radiation Physics and Chemistry, 1986. 27(3): p. 241-243.
20. Huang, J., *Carbonate Radicals in Natural Waters*, in *Department of Chemistry*. 2000, University of Toronto: Toronto.
21. Larson, R.A. and R.G. Zepp, *Reactivity of the carbonate radical with aniline derivatives.* Environmental Toxicology and Chemistry, 1988. 7(4): p. 265-274.
22. Bisby, R.H., et al., *Time-resolved resonance Raman spectroscopy of the carbonate radical.* Journal of the Chemical Society-Faraday Transactions, 1998. 94(15): p. 2069-2072.
23. Zepp, R.G., J. Hoigne, and H. Bader, *Nitrate-induced photooxidation of trace organic-chemicals in water.* Environmental Science & Technology, 1987. 21(5): p. 443-450.
24. Zepp, R.G., B.C. Faust, and J. Hoigne, *HYDROXYL RADICAL FORMATION IN AQUEOUS REACTIONS (PH 3-8) OF IRON(II) WITH HYDROGEN-PEROXIDE - THE PHOTO-FENTON REACTION.* Environmental Science & Technology, 1992. 26(2): p. 313-319.
25. Zafiriou, O.C., *Sources and reactions of OH and daughter radicals in seawater.* Journal of Geophysical Research, 1974. 79(30): p. 4491-4497.
26. Mill, T., D.G. Hendry, and H. Richardson, *Free-radical oxidants in natural-waters.* Science, 1980. 207(4433): p. 886-887.
27. Huang, J.P. and S.A. Mabury, *Steady-state concentrations of carbonate radicals in field waters.* Environmental Toxicology and Chemistry, 2000. 19(9): p. 2181-2188.
28. Dimmock, N.J.a.E., A J and Leppard K N, *Introduction to modern virology*. 7th ed. 2007, Oxford: Blackwell Publishing.
29. Koonin, E.V., T.G. Senkevich, and V.V. Dolja, *The ancient Virus World and evolution of cells.* Biology Direct, 2006. 1.
30. Thiel, T.K., *Hepatitis A vaccination.* American Family Physician, 1998. 57(7): p. 1500-1500.
31. Ryan, K.J.a.R., C.G., *Sherris Medical Microbiology*. 5 ed. Chapter 13 Hepatitis viruses. 2010, New York: The McGraw-Hill companies.
32. Helantera, I., et al., *Viral Impact on Long-term Kidney Graft Function.* Infectious Disease Clinics of North America, 2010. 24(2): p. 339-+.
33. Lin, C.Y., et al., *The Emerging Importance of Norovirus as the Etiology of Pediatric Gastroenteritis in Taipei.* Journal of Microbiology Immunology and Infection, 2010. 43(2): p. 105-110.
34. Snijder, E.J., et al., *Unique and conserved features of genome and proteome of SARS-coronavirus, an early split-off from the coronavirus group 2 lineage.* Journal of Molecular Biology, 2003. 331(5): p. 991-1004.

35. Fraise, A.P., Lambert, P.A. and Maillard, J-Y., ed. *Russell, Hugo and Ayliffe's principles and practice of disinfection*. Viricidal activity of biocides, ed. J.-Y. Maillard. 2004, Blackwell Publishing Oxford. 272-323.
36. Valegård, K.L., L., Fridborg, K. and Unge, T, *.The three-dimensional structure of the bacterial virus MS2.* Nature, 1990. 345: p. 36-41.
37. Silverma.Pm and Valentin.Rc, *RNA injection step of bacteriophage F2 infection.* Journal of General Virology, 1969. 4: p. 111-&.
38. Havelaar, A.H., M. Vanolphen, and Y.C. Drost, *F-specific RNA bacteriophages are adequate model organisms for enteric viruses in fresh-water.* Applied and Environmental Microbiology, 1993. 59(9): p. 2956-2962.
39. Davies, M.J., *Singlet oxygen-mediated damage to proteins and its consequences.* Biochemical and Biophysical Research Communications, 2003. 305(3): p. 761-770.
40. Sanger, F., Air, G.M., Barrell, B.G., Brown, N.L., Coulson, A.R., Fiddes, C.A., Hutchison, C.A., Slocombe, P.M. and Smith, M., *Nucleotide sequence of bacteriophage phi X174 DNA.* Nature, 1977. 265(5596): p. 687–695.
41. Fraenkel-Conrat, H.a.W., R.R., ed. *Comprehensive Virology*. Structure and function of RNA bacteriophages, ed. W. Fiers. Vol. 13. 1979, Plenum Publishing Corporation: New York.
42. Simonet, J. and C. Gantzer, *Inactivation of poliovirus 1 and F-specific RNA phages and degradation of their genomes by UV irradiation at 254 nanometers.* Applied and Environmental Microbiology, 2006. 72(12): p. 7671-7677.
43. Kohn, T., Nieto, J.I, Pescon, B.M. and Wigginton, K.R., *Disinfection of viruses in surface water by reactive oxygen species*, in *Annual Assembly of the Swiss Society for Microbiology*. 2009: Lausanne.
44. Kutter, K.a.S., A., ed. *Bacteriophages: Biology and Applications*. Appendix, ed. K. Carlson. 2005, CRC Press: Boca Raton.
45. The Resource for Biocomputing, V., and Informatics (RBVI), *Virus Capsid Images*, University of California.
46. Canonica, S., et al., *Photosensitizer method to determine rate constants for the reaction of carbonate radical with organic compounds.* Environmental Science & Technology, 2005. 39(23): p. 9182-9188.
47. Porter, G.a.S., P, *Reactivity of the excited states of aromatic ketones.* Pure and Applied Chemistry, 1964. 9(4): p. 499-505.
48. Waite, M.R.F., Pfefferk.Er, and D.T. Brown, *INHIBITION OF SINDBIS VIRUS RELEASE BY MEDIA OF LOW IONIC-STRENGTH - ELECTRON-MICROSCOPE STUDY.* Journal of Virology, 1972. 10(3): p. 537-&.
49. Mendonca, A.F., T.L. Amoroso, and S.J. Knabel, *Destruction of gram-negative food-borne pathogens by high pH involves disruption of the cytoplasmic membrane.* Applied and Environmental Microbiology, 1994. 60(11): p. 4009-4014.
50. Wilkinson, F., Helman, W.P. and Ross, A.B., *Quantum yields for the phonsensitized formation of the lowest electronically excited singlet state of molecular oxygen in solution.* Journal of Physical and Chemical Reference Data, 1993. 22(1): p. 113-262.
51. Thomsen, C.L., J. Thogersen, and S.R. Keiding, *Ultrafast charge-transfer dynamics: Studies of p-nitroaniline in water and dioxane.* Journal of Physical Chemistry A, 1998. 102(7): p. 1062-1067.
52. Ma, H.J., et al., *Steady-state and transient photolysis of p-nitroaniline in acetonitrile.* Journal of Photochemistry and Photobiology a-Chemistry, 2009. 202(1): p. 67-73.
53. Loeff, I., et al., *charge-transfer and reactivity of n-pi-asterisk and pi-pi-asterisk organic triplets, including anthraquinonesulfonates, in interactions with inorganic anions - a comparative-study*

based on classical marcus theory. Journal of the American Chemical Society, 1993. 115(20): p. 8933-8942.

54. Huie, R.E., C.L. Clifton, and P. Neta, *Electron-transfer reaction-rates and equilibria of the carbonate and sulfate radical-anions.* Radiation Physics and Chemistry, 1991. 38(5): p. 477-481.
55. Buxton, G.V.a.G., C.L., *Critical reviews of rate constants for reactions of hydrated electrons, hydrogen atoms and hydroxyl radicals (•OH/•O-) in aqueous solution.* Journal of Physical and Chemical Reference Data, 1988. 17(2): p. 513-886.
56. Umschlag, T. and H. Herrmann, *The carbonate radical (HCO3 center dot/CO3-center dot) as a reactive intermediate in water chemistry: Kinetics and modelling.* Acta Hydrochimica Et Hydrobiologica, 1999. 27(4): p. 214-222.
57. Canonica, S. and H.U. Laubscher, *Inhibitory effect of dissolved organic matter on triplet-induced oxidation of aquatic contaminants.* Photochemical & Photobiological Sciences, 2008. 7(5): p. 547-551.
58. Lilie, J., R.J. Hanrahan, and A. Henglein, *O- transfer-reactions of carbonate radical-anion.* Radiation Physics and Chemistry, 1978. 11(5): p. 225-227.
59. Canonica, S., B. Hellrung, and J. Wirz, *Oxidation of phenols by triplet aromatic ketones in aqueous solution.* Journal of Physical Chemistry A, 2000. 104(6): p. 1226-1232.
60. Olsthoorn, R.C.L., et al., *Nucleotide-sequence of a single-stranded rna phage from pseudomonas-aeruginosa - kinship to coliphages and conservation of regulatory rna structures.* virology, 1995. 206(1): p. 611-625.
61. Zerda, K.S., et al., *Adsorption of viruses to charge-modified silica.* Applied and Environmental Microbiology, 1985. 49(1): p. 91-95.
62. Elango, T.P., et al., *Radiation chemical studies of nickel-glycine reaction with carbonate radical.* journal of radioanalytical and nuclear chemistry-articles, 1988. 125(1): p. 151-155.